Colloid Polym Sci 274:227–238 (1996)

ORIGINAL CONTRIBUTION

T.D. Gurkov
P.A. Kralchevsky
K. Nagayama

Formation of dimers in lipid monolayers

Received: 15 March 1995
Accepted: 15 September 1995

T.D. Gurkov · Prof. P.A. Kralchevsky (✉)
Faculty of Chemistry
University of Sofia
1 James Boucher Ave.
1126 Sofia, Bulgaria

K. Nagayama
Protein Array Project
ERATO
JRDC
5-9-1 Tokodai
Tsukuba 300-26, Japan

Abstract In this work, we analyse theoretically the hypothesis that zwitterionic lipids form dimers in adsorption monolayers on water/hydrocarbon phase boundary. A dimer can be modelled as a couple of lipid molecules whose headgroup lateral dipole moments have antiparallel orientation. Properties including surface pressure, chemical potentials and activity coefficients are deduced from a general expression for the free energy of the monolayer. The theoretical model is in a good agreement with experimental data for surface pressure and surface potential of lipid monolayers. The results favour the hypothesis about formation of dimers in equilibrium with monomers, with the amount of the species depending on the area per molecule and temperature. The reaction of dimerisation turns out to be exothermic with a heat of about 2.5 kT per dimer. The results may be applied to the molecular models of membrane structures and mechanisms.

Key words Lipid dimers – lipid monolayers – membranes of lipids – surface potential of lipids – surface pressure of lipids

Introduction

The lipid bilayers are constituent material of the biomembranes in every living cell. The study of their structure and properties provokes a permanent research interest. A deeper understanding in this field can be achieved by a comparative study of a simpler system – the lipid adsorption monolayers.

A comprehensive experimental investigation of phospholipid adsorption monolayers at oil/water interface has been published in Refs. [1–7], including $\Pi(a)$ isotherms (Π is surface pressure and a is area per lipid molecule), and ΔV-potential measurements. An important conclusion from these experiments is that the surface pressure is affected neither by the length of the hydrophobic chains (below any surface phase transition), nor by the electrolyte concentration [7]. In addition, the data show large deviations from the ideal value $\Pi a/(kT) = 1$ (k is the Boltzmann constant and T is temperature), which are independent of the chain length in the C_{14} to C_{22} range. This implies that the lipid hydrocarbon chains do not contribute to the nonideality of Π. The latter therefore depends only on the lateral headgroup interactions [7], which in turn are determined by the magnitude and orientation of the dipole moments of the zwitterionic headgroups.

As discussed in refs. [8] and [9], x-ray crystallography and neutron scattering experiments show that the headgroups of phosphatidylcholines and phosphatidylethanolamines have similar orientations, essentially parallel to the plane of the interface (see Fig. 1a). In addition, it has been recognised that the lipid headgroup possesses a significant *lateral* dipole moment, which is parallel to the surface [10–12]. There is also non-zero *normal* resultant of

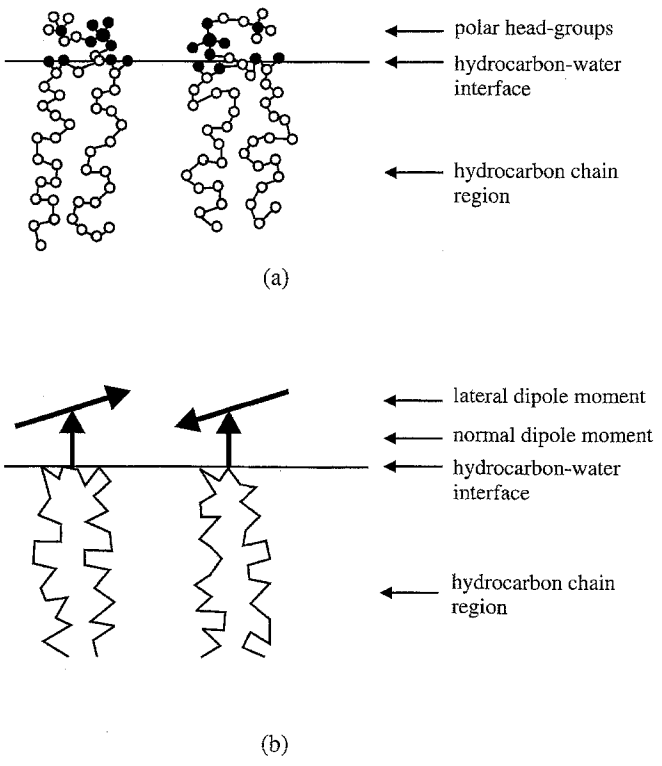

Fig. 1 Sketch of two lipid molecules adsorbed on hydrocarbon-water interface: a) Real scale drawing; b) The polar heads are modelled to have net normal and lateral dipole moments

the headgroup dipole moment which is directed toward the water phase but is smaller in magnitude than the contrariwise oriented dipole moment coming from the water molecules which surround the polar head [12]. Surface potential measurements gave evidence for the latter fact [10–12]; it is virtually impossible to calculate the lateral dipole-dipole interactions by using only structure data for the lipid molecules.

An admissible theoretical model focused on the major features of the headgroup structure is to ascribe the total interaction to *net* lateral and normal dipole moments resulting from a superposition of different factors. In the framework of this model we sketch a lipid molecule like a weather-cock (Fig. 1b) built up from the normal and lateral dipole moments. These dipole moments can be determined by comparing the predictions of the model with the experiment.

One can expect that the normal dipole moments of two adsorbed lipids (Fig. 1) will always repel each other, being *parallel*, whereas the lateral dipole moments will tend to acquire *antiparallel* orientation which corresponds to attraction. If at small lipid–lipid separations the attraction prevails over the repulsion, the two lipid molecules will join together to form a dimer. This hypothesis is verified in the next section of this article, where experimental $\Pi(a)$-isotherms from refs. [1] and [7] are analysed by means of the two-dimensional van der Waals equation of state. We note in advance that the results provide a clear indication about the dimer formation in relatively *concentrated* lipid monolayers (area per molecule between 75 and 250 Å^2).

Next, we extend the van der Waals approach to *more diluted* monolayers, which are treated as binary mixtures of monomers and dimers. Expressions for the chemical potentials and activity coefficients of the lipid monomers and dimers are derived from the concentration dependence of the monolayer free energy. Then by using the mass action law the molar fractions of monomers and dimers are determined as functions of the surface concentration. By fitting the experimental $\Pi(a)$ data we obtain values for the parameters of the system, including the energy (heat) of dimer formation and the interaction parameter for two monomers.

We should say from the very beginning that our relatively simple theoretical model is not able to explain the behaviour of the lipid monolayers for all surface concentrations, and especially the phase transition which has been observed experimentally in concentrated monolayers [1]. Indeed, the validity of the *two-dimensional* van der Waals equation of state is restricted to areas per molecule for which the lipids can be regarded as *interacting hard discs in thermal motion*, modelling essentially the lipid headgroups (but not the hydrocarbon tails). Therefore, one should not expect this equation to be able to describe the phase transition at high surface concentrations. The latter is most probably due to structural changes in the hydrocarbon chain region of the lipid monolayer, which may be also accompanied by some changes in the structure of the zwitterionic hydration shells. The van der Waals approach and our theoretical model are supposed to be valid when the lipid-lipid interactions are dominated by the headgroup-headgroup interactions without changes in the molecular structure. As shown below, such turns out to be the case of lipid dimerisation.

Concentrated lipid monolayers

Our first step is to verify the hypothesis about the formation of lipid dimers in adsorption monolayers by interpreting data from refs. [1, 7] for the surface pressure of concentrated lipid monolayers (area per molecule between 75 and 250 Å^2), below the surface phase transition to closely packed monolayer. On that purpose we will make use of the two-dimensional van der Waals equation [13, 14]

$$\left(\Pi + \frac{c}{\alpha^2}\right)(\alpha - \beta) = kT \,. \tag{1.1}$$

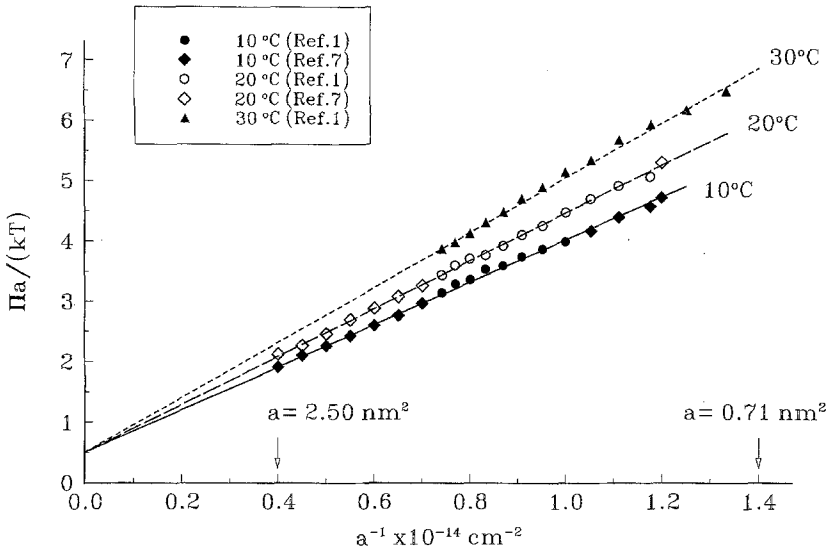

Fig. 2 Plot of $\Pi a/(kT)$ vs. a^{-1} for 1,2-distearoyl lecithin at the *n*-heptane/aqueous NaCl solution interface, at three different temperatures (Π is surface pressure and a is area per molecule). The symbols denote experimental data, taken from Fig. 1 in ref. [1] and from Figs. 9 and 10 in ref. [7]

Here, $\alpha = va$ is the area per aggregate ($v = 1$ for monomers, $v = 2$ for dimers, etc.); $\beta = vb$ is the excluded area per aggregate with b being the excluded area per monomer; c accounts for the interaggregate interactions (repulsive and attractive). As demonstrated by Landau and Lifshitz [13], the van der Waals equation, Eq. (1.1), is a successful interpolation formula, which behaves correctly for both low and high concentrations. Moreover, the parameters β and c can be expressed through integrals of the interaction energy between the aggregates, $u(r)$, [13]:

$$\beta = \pi \int_0^{r_c} \left(1 - e^{-\frac{u(r)}{kT}}\right) r dr \approx \frac{\pi}{2} r_c^2$$

$$c = -\pi kT \int_{r_c}^{\infty} \left(1 - e^{-\frac{u(r)}{kT}}\right) r dr \approx -\pi \int_{r_c}^{\infty} u(r) r dr \,, \qquad (1.2)$$

where r_c is the interparticle center-to-center distance at contact, i.e., $u(r) \to \infty$ for $r < r_c$.

The expansion of Eq. (1.1) in series for $\alpha \gg \beta$ yields

$$\frac{\Pi a}{kT} = \frac{1}{v} + \frac{b}{v}\left(1 - \frac{c}{vbkT}\right)\frac{1}{a} + O\left(\frac{b^2}{a^2}\right). \qquad (1.3)$$

From the intercept of the plot of $\Pi a/(kT)$ vs. $1/a$ one can determine v.

Figure 2 represents the plot of $\Pi a/(kT)$ vs. $1/a$ for 1,2-distearoyl lecithin at *n*-heptane/aqueous NaCl solution interface in the range of a from 250 to 75 Å^2; the data are taken from Fig. 1 in ref. [1] and from Figs. 9 and 10 in ref. [7]. The straight lines are drawn in accordance with Eq. (1.3) by means of the least squares method. The calculated values of the line intercepts, slopes, their standard deviations and the correlation coefficients are listed in Table 1. One sees that for all temperatures the intercept is close to 0.5 as it is expected for dimers (for monomers the intercept must be equal to 1). Without being a direct proof, this finding favours the hypothesis that the concentrated lipid monolayers (and possibly bilayers) are composed of lipid dimers. Moreover, below we demonstrate that the determined values of the slope (Table 1) are also consonant with this hypothesis.

Table 1 Data for the slope, intercept and the correlation coefficient of the linear plots of $\Pi a/(kT)$ vs. $1/a$ at different temperatures, see Fig. 2.

Temperature °C	Intercept	Slope $\times 10^{14}$, cm^2	Correlation Coefficient
10	0.541 ± 0.034	3.480 ± 0.041	0.9988
20	0.513 ± 0.029	3.948 ± 0.035	0.9994
30	0.524 ± 0.088	4.556 ± 0.088	0.9980

Let us first estimate the excluded area per lipid molecule, b, which takes part in the expression for the slope, see Eq. (1.3). One can expect that the excluded area per molecule is equal to the partial molecular area for the bilayer in its most condensed liquid state, which is about 40 Å^2 for all temperatures studied [1]. With $b = 40$ Å^2 and $v = 2$ from the slope of the respective line one estimates

$$c = -6.0 \times 10^{-34}\ \mathrm{J \cdot cm^2} \quad (T = 20\,^\circ\mathrm{C}). \qquad (1.4)$$

On the other hand, considering the dimers as mutually parallel dipoles of dipole moment p_d one has $u(r) = p_d^2/(\varepsilon r^3)$, which after substitution in Eq. (1.2) yields

$$c = -\frac{\pi p_d^2}{\varepsilon r_c} = \frac{-\varepsilon}{4\pi r_c}(a\Delta V)^2 \,, \qquad (1.5)$$

where ε is dielectric permittivity. At the last step we connected the dipole moment of the adsorbed molecules

with the surface (Volta) potential produced by them: $\Delta V = (4\pi p_d)/(\varepsilon\alpha)$; note that $\alpha = 2a$. The surface potential ΔV is liable to a direct measurement. The experiments [5–7] show that the product $a\Delta V$ is almost constant (independent of a) for a lipid monolayer at a given temperature. Thus for $T = 20\,^{\circ}C$ the experiment yields $a\Delta V = 2.34 \times 10^{-15}\ V \cdot cm^2$. The substitution of the latter value in Eq. (1.5), along with $\varepsilon = 78$ and $r_c \approx (4b/\pi)^{1/2} = 7.1$ Å, gives $c = -5.3 \times 10^{-34}\ J \cdot cm^2$, which is close to the experimental value, see Eq. (1.4) above. (Note that ΔV in Eq. (1.5) is expressed in CGSE units, i.e. the value of ΔV in volts must be divided by 300.)

One can conclude that the values of the slope and intercept of the lines in Fig. 1 (see also Table 1) are in agreement with the hypothesis that the lipid molecules in relatively concentrated monolayers exist in the form of dimers. This finding encourages us to extend the study to the case of more diluted monolayers, in which a coexistence of lipid monomers and dimers is to be expected.

Theoretical model of lipid monolayers

Below we treat a lipid monolayer as a binary mixture of monomers and dimers. Our final goal is to determine the dimer surface concentration as a function of the total lipid surface concentration, and to calculate the heat (energy) of dimer formation. With this end in view let us first consider a diluted binary mixture.

For low lipid surface concentration one can use the virial expansion for the free energy F. By using the standard methods of statistical mechanics [13–15] one can derive

$$F = F_{id} + \frac{kT}{A}\left[N_1^2 B_{11}(T) + 2N_1 N_2 B_{12}(T) + N_2^2 B_{22}(T)\right] + \cdots \qquad (2.1)$$

– see also Eq. (11.30) in ref. [16]. Here, F is the free energy of the lipid monolayer, which is treated as a *two-dimensional* binary mixture of monomers and dimers; A is the area of the monolayer; N_1 and N_2 are the numbers of monomers and dimers, respectively; $B_{ij}(T)$ are the second virial coefficients [14]:

$$B_{ij} = \pi \int_0^\infty \left(1 - e^{-\frac{u_{ij}}{kT}}\right) r dr, \quad i,j = 1,2 \qquad (2.2)$$

$u_{ij}(r)$ is the interaction energy of a molecule of component i with a molecule of component j separated at a distance r. (u_{ij} is an angle averaged free energy in accordance with the potential distribution theorem [17].) F_{id} in Eq. (2.1) stands for the free energy of an *ideal* two-dimensional binary mixture [14]:

$$F_{id} = -kT\left[N_1 \ln\left(\frac{Ae}{\Lambda_1^2 N_1}\right) + N_2 \ln\left(\frac{Ae}{\Lambda_2^2 N_2}\right)\right], \qquad (2.3)$$

where $\Lambda_i = h/(2\pi m_i kT)^{1/2}$ for a particle of mass m_i; h is the Planck constant, e is the base of the natural logarithm. Further, we assume that each adsorbed particle of a given kind (monomer or dimer) excludes some area, i.e.

$$u_{ij} = +\infty \quad \text{for} \quad r < r_{ij}, \quad i,j = 1,2\,, \qquad (2.4)$$

where r_{ij} is the interparticle center-to-center distance at contact. Then, following the classical van der Waals approach, one can separate the contributions of the area exclusion and the long-range forces (electrostatic, van der Waals, etc.) in the virial coefficients [13, 14]:

$$B_{ij} = b_{ij} - \frac{c_{ij}}{kT}, \quad i,j = 1,2\,, \qquad (2.5)$$

where

$$b_{ij} = \pi \int_0^{r_{ij}} \left(1 - e^{-\frac{u_{ij}}{kT}}\right) r dr = \frac{\pi}{2} r_{ij}^2 \qquad (2.6)$$

$$c_{ij} = -\pi kT \int_{r_{ij}}^\infty \left(1 - e^{-\frac{u_{ij}}{kT}}\right) r dr \approx -\pi \int_{r_{ij}}^\infty u_{ij}(r) r\, dr\,. \qquad (2.7)$$

The substitution of Eq. (2.5) into Eq. (2.1) yields

$$F = F_{id} + \frac{N^2}{A}(bkT - c)\,, \qquad (2.8)$$

where

$$b = x_1^2 b_{11} + 2x_1 x_2 b_{12} + x_2^2 b_{22} \qquad (2.9)$$

$$c = x_1^2 c_{11} + 2x_1 x_2 c_{12} + x_2^2 c_{22}\,, \qquad (2.10)$$

with x_1 and x_2 being the molar fractions of the two components:

$$x_1 = \frac{N_1}{N}, \qquad x_2 = \frac{N_2}{N}, \quad N = N_1 + N_2\,. \qquad (2.11)$$

Equation (2.8) is analogous to Eq. (76.3) in ref. [13]. Then, following the heuristic scheme proposed by Landau and Lifshitz [13], we obtain a counterpart of their Eq. (76.6) for a two-dimensional binary mixture:

$$F = F_{id} - NkT \ln\left(1 - \frac{Nb}{A}\right) - \frac{N^2 c}{A}. \qquad (2.12)$$

In fact, Eq. (2.12) is an interpolation formula which connects the limiting cases of diluted monolayer ($A \gg Nb$) and condensed monolayer ($A \to Nb$). Indeed, for a diluted monolayer one can easily deduce Eq. (2.8) from Eq. (2.12). On the other hand, for condensed monolayer ($A \to Nb$) the logarithmic term in Eq. (2.12) infinitely increases,

which is an indication for the *finite* compressibility of the mixture [13].

The surface pressure, Π, can be calculated by differentiating the free energy [14]

$$\Pi = -\left(\frac{\partial F}{\partial A}\right)_{T,N_1,N_2} . \tag{2.13}$$

From Eqs. (2.3), (2.12) and (2.13) one derives

$$\left(\Pi + \frac{N^2 c}{A^2}\right)(A - Nb) = NkT , \tag{2.14}$$

which is a two-dimensional version of the van der Waals equation of state. The fact that we deal with a binary *mixture* is accounted for by the dependence of b and c on the composition, see Eqs. (2.9) and (2.10). Disregarding the latter dependence, Eq. (2.14) is known in the literature [14]. Therefore, it might seem that we arrived at a trivial result. However, as demonstrated below, from the more general expression for the free energy, Eq. (2.12), one can deduce quite nontrivial results for the concentration dependencies of the properties of the system. In particular, expressions for the *activity coefficients* of the species can be derived, which give the key to a quantitative description of the monomer-dimer equilibrium.

Activity coefficients of lipids in adsorption monolayer

The chemical potentials of the species can be calculated by differentiation of the free energy:

$$\mu_1 = \left(\frac{\partial F}{\partial N_1}\right)_{T,A,N_2} , \qquad \mu_2 = \left(\frac{\partial F}{\partial N_2}\right)_{T,A,N_1} \tag{3.1}$$

As usual, the subscripts 1 and 2 denote monomers and dimers, respectively. The differentiation of Eq. (2.12), along with Eqs. (2.9)–(2.11), yields

$$\mu_1 = \mu_{10}(T) + kT\ln(\Gamma_1\gamma_1), \quad \mu_2 = \mu_{20}(T) + kT\ln(\Gamma_2\gamma_2) \tag{3.2}$$

where

$$\Gamma_1 = N_1/A \quad \text{and} \quad \Gamma_2 = N_2/A \tag{3.3}$$

are the surface concentrations (adsorptions) of the two components and

$$\gamma_i \equiv (1 - \Gamma b)^{-1} \exp\left[\frac{\Gamma}{1 - \Gamma b}(2x_i b_{ii} + 2x_j b_{ji} - b) - \frac{2}{kT}(\Gamma_i c_{ii} + \Gamma_j c_{ji})\right] \tag{3.4}$$

$$i, j = 1, 2, \qquad j \neq i$$

are the activity coefficients; $\Gamma = \Gamma_1 + \Gamma_2$ is the total adsorption, μ_{10} and μ_{20} are standard chemical potentials, which are independent of Γ_1 and Γ_2; besides, $b_{21} = b_{12}$ and $c_{21} = c_{12}$ by definition. If equilibrium between monomers and dimers is established, one can write [14]

$$\mu_2 = 2\mu_1 . \tag{3.5}$$

The substitution of Eq. (3.2) into Eq. (3.5) yields

$$\frac{\Gamma_2\gamma_2}{\Gamma_1^2\gamma_1^2} = K(T) \equiv \exp\left(-\frac{\mu_{20} - 2\mu_{10}}{kT}\right), \tag{3.6}$$

where K is the reaction constant (function of temperature only).

In the experiments the dependence of the surface pressure Π on the average area per lipid molecule, a, is determined. As the adsorbed lipids are supposed to exist in the form of monomers and dimers, a can be expressed in the form

$$a = 1/(\Gamma_1 + 2\Gamma_2) , \tag{3.7}$$

Note that Eqs. (3.6), (3.7) and (3.4) (for $i = 1, 2$) provide a set of four equations determining the values of the four variables Γ_1, Γ_2, γ_1 and γ_2 for each given value of a, if only the parameters b_{11}, b_{12}, b_{22}, c_{11}, c_{12}, c_{22} and K are known for the respective temperature. Then from the van der Waals equation, Eq. (2.14), which can be transformed to read

$$\frac{\Pi a}{kT} = \frac{1}{1 + x_2}\left(\frac{1}{1 - \Gamma b} - \frac{\Gamma c}{kT}\right) \quad \left(\Gamma = \frac{1}{(1 + x_2)a}\right), \tag{3.8}$$

($x_2 = \Gamma_2/\Gamma$), one can calculate the theoretical dependence Π vs. a. The next section is devoted to the determination of the parameters of the model.

When solving the problem numerically we met a computational difficulty, viz., the substitution of Eqs. (3.4) and (3.7) into Eq. (3.6) leads to an *implicit* equation for x_2 having several roots in the interval $0 \leq x_2 \leq 1$. Then the problem of which root is physical arises. To circumvent this problem we used series expansions for large values of a, which provide *explicit* expressions for Γ and x_2:

$$\Gamma = \Gamma_{(1)}a^{-1} + \Gamma_{(2)}a^{-2} + \Gamma_{(3)}a^{-3} + \cdots \tag{3.9}$$

$$x_2 = y_1 a^{-1} + y_2 a^{-2} + y_3 a^{-3} + \cdots \tag{3.10}$$

The coefficients $\Gamma_{(i)}$ and y_i ($i = 1, 2, 3$) are determined and listed in the Appendix. Series expansions can be derived also for the activity coefficients. In particular, in first approximation one has

$$\gamma_1 = 1 + \frac{2}{a}\left(b_{11} - \frac{c_{11}}{kT}\right) + O(a^{-2});$$

$$\gamma_2 = 1 + \frac{2}{a}\left(b_{12} - \frac{c_{12}}{kT}\right) + O(a^{-2}) .$$

Colloid & Polymer Science, Vol. 274, No. 3 (1996)

The substitution of the expansions, Eqs. (3.9) and (3.10), into Eq. (3.8), along with Eqs. (2.9) and (2.10), determines explicitly the theoretical dependence of Π vs. a. Of course, these expansions cannot be applied for high surface concentrations. However, the experimental data interpreted below (Fig. 5) are measured within a range of a that allows the expansions to be used.

Determining the parameters of the model

So far, we have seven unknown parameters: b_{11}, b_{12}, b_{22}, c_{11}, c_{12}, c_{22}, and the equilibrium constant $K(T)$. They are too many for all of them to be treated as adjustable parameters. Fortunately, some physical considerations presented below allow us to estimate (more or less accurately) 4 of these parameters.

In the van der Waals approach b_{11} is the minimum possible area per lipid molecule. In the most condensed state of the monolayers studied in ref. [1] the area per molecule was 40 Å^2 irrespective of the temperature. Therefore, as before, we assume

$$b_{11} = 40 \text{ Å}^2 \tag{4.1}$$

for lecithin. On the same grounds it is natural to adopt

$$b_{22} = 2b_{11} = 80 \text{ Å}^2 \tag{4.2}$$

for the minimum area occupied by a dimer. Further, in the van der Waals model b_{ij} is identified as $\pi r_{ij}^2/2$, which is half the area of a disk of diameter r_{ij}, cf. Eq. (2.6). Then it is usually supposed that $r_{12} = (r_{11} + r_{22})/2$ (see ref. [14], section 15.3), and consequently

$$b_{12} = \left[\frac{1}{2}(\sqrt{b_{11}} + \sqrt{b_{22}})\right]^2 = 58.3 \text{ Å}^2 . \tag{4.3}$$

We should note that below we deal with areas per molecule varying between 200 and 1000 Å^2, i.e. with $a \gg b_{11}$. For this reason, we can expect that the results are not so sensitive with respect to the values of the parameters b_{11}, b_{12} and b_{22}.

Since the normal dipole moments of two lipids *coupled in a dimer* are assumed to be parallel, whereas the lateral dipole moments – to be antiparallel, one can expect that the dimer-dimer interaction is dominated by the repulsion between the two couples of parallel normal dipole moments, i.e. $u_{22} = (2p)^2/(\varepsilon r^3)$ [18]. Here, p is the normal resultant of the dipole moment per lipid monomer; ε is dielectric permittivity. With this expression for u_{22}, from Eq. (2.7), one estimates

$$c_{22} = -\frac{4\pi p^2}{\varepsilon r_{22}} . \tag{4.4}$$

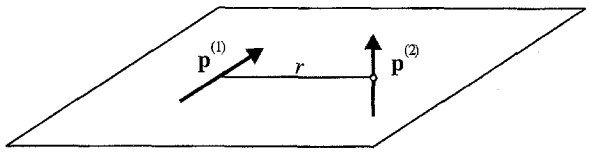

Fig. 3 Sketch of a lateral dipole moment of a lipid molecule ($\mathbf{p}^{(1)}$) and a neighbouring normal dipole moment of a dimer ($\mathbf{p}^{(2)}$)

Next we consider the monomer–dimer interaction.The normal dipole moment of a dimer interacts with both the normal and the lateral dipole moments of a monomer. In general, the energy of interaction of two point dipoles of moments $\mathbf{p}^{(1)}$ and $\mathbf{p}^{(2)}$ is given by the expression [18]

$$u_p = \frac{1}{\varepsilon r^3}\left[\mathbf{p}^{(1)}\cdot\mathbf{p}^{(2)} - \frac{3}{r^2}(\mathbf{p}^{(1)}\cdot\mathbf{r})(\mathbf{p}^{(2)}\cdot\mathbf{r})\right], \tag{4.5}$$

where $\mathbf{r}$ is the vector connecting the positions of the two dipoles. If $\mathbf{p}^{(1)}$ is the monomer lateral dipole moment and $\mathbf{p}^{(2)}$ is the dimer normal dipole moment, the sketch in Fig. 3 shows that $\mathbf{p}^{(1)}\cdot\mathbf{p}^{(2)} = 0$ and $\mathbf{p}^{(2)}\cdot\mathbf{r} = 0$. Then Eq. (4.5) yields $u_p = 0$. Of course, the lipid dipoles are not point dipoles, and their positions might be somewhat different from those depicted in Fig. 3. Nevertheless, the above considerations show that the lateral–normal dipole interaction can be expected to be much weaker compared to the normal–normal dipole interaction. Then one can estimate c_{12} similarly to c_{22}, viz.

$$c_{12} = -\frac{2\pi p^2}{\varepsilon r_{12}} . \tag{4.6}$$

From Eqs. (2.6), (4.4) and (4.6) one derives

$$c_{12} = \frac{1}{2}\sqrt{\frac{b_{22}}{b_{12}}}\, c_{22} . \tag{4.7}$$

Finally, let us consider the monomer–monomer interaction. One can foresee that both normal–normal and lateral–lateral dipole–dipole interactions will be important. The contribution of the normal–normal interaction in c_{11} can be estimated with an expression of the type of Eq. (4.4) or (4.6). However, it is not easy to evaluate the lateral–lateral dipole interaction. Indeed, for large intermolecular separation one can expect correlation between the two Brownian rotators (the two "weather-cocks" sketched in Fig. 1b); this would yield an interaction energy decaying as r^{-6}, as it is for the Keesom interaction [17]. However, at close approach the two lateral dipoles will tend to form an antiparallel pair since their thermal rotation will be hindered by steric effects; in this case strong Coulomb attraction has to be expected. At intermediate distances some transition from Coulomb to Keesom

interaction should take place. This qualitative picture does not allow a quantitative estimate of c_{11}. That is why we treat c_{11} as an adjustable parameter, whose value is obtained by comparing theory with experiment. The values of p and ε in Eqs. (4.4) and (4.6) are not accurately known too. For that reason, we treat also c_{22} as an adjustable parameter, whereas c_{12} is calculated by means of Eq. (4.7).

In summary, we use three adjustable parameters, $K(T)$, c_{11} and c_{22}, with the other four model parameters, b_{11}, b_{22}, b_{12}, and c_{12}, being determined by Eqs. (4.1), (4.2), (4.3) and (4.7), respectively.

To find $K(T)$, c_{11} and c_{22} for a given temperature we used the least squares method, i.e. we minimised numerically the function

$$\Phi(c_{11}, c_{22}, K) = \sum_n [\Pi_n - \Pi(a_n; c_{11}, c_{22}, K)]^2 , \qquad (4.8)$$

where (a_n, Π_n), $n = 1, 2, 3, \ldots$, are the points of the experimental $\Pi(a)$-isotherm and the theoretical function $\Pi(a; c_{11}, c_{22}, K)$ is given by Eqs. (3.8)–(3.10).

Before presenting the numerical results let us discuss briefly our expectations. Figure 4 presents schematically the expected dependence of the energy of interaction between two lipid molecules (like those depicted in Fig. 1) as a function of the intermolecular separation, r (averaging over the angular coordinates is assumed). Of course, the lipid–lipid interaction energy, $u_{11}(r)$, cannot be directly extracted from experimental $\Pi(a)$ isotherms. We can determine ΔE, which characterises the depth of the minimum of u_{11}, and c_{11}, which is proportional to an integral of u_{11}, see Eq. (2.7). The positive total value of the hatched area in Fig. 4 gives an indication that the contribution of repulsion in c_{11} prevails over the contribution of attraction.

At large distances the repulsion between the normal dipoles decays as $1/r^3$, whereas the attraction between the lateral dipole moments involved in Brownian rotation decays faster, as $1/r^6$ (the Keesom interaction). Hence, one can expect that c_{11} is dominated by the repulsion. On the other hand, we cannot anticipate in advance whether ΔE is positive or negative.

Negative ΔE corresponding to the configuration depicted in Fig. 4 would mean that the dimerisation is an *exothermic* reaction, i.e., the lipid dimer is a *stable* formation present even at low surface concentrations.

On the contrary, positive ΔE (the value of u_{11} at the minimum is positive) would mean that the dimerisation is an *endothermic* reaction, and that the lipid dimer is a *metastable* formation which can appear only when the surface concentration is high enough.

The answers of these and other questions, as well as our conclusions about the reliability of the hypothesis for lipid dimerisation, can be found below.

Fig. 4 Schematic plot of the energy of interaction between two lipid molecules

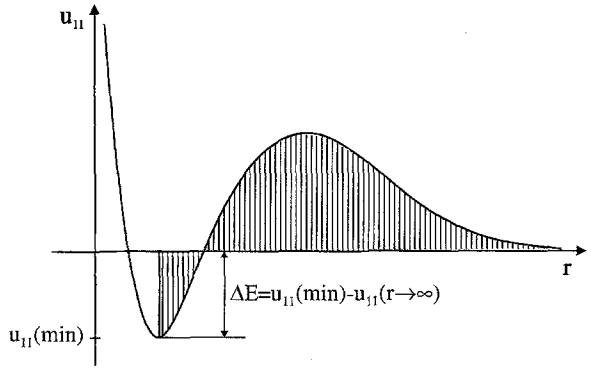

Comparison of theory and experiment

We fit the $\Pi(a)$ data for di-C_{18}-lecithin at the *n*-heptane/aqueous NaCl interface, published in ref. [2] (Fig. 5 therein). The area per lipid molecule, a, ranges from about 200 to 1000 Å^2, which justifies the application of series expansions at small a^{-1}, see above. Experimental results for five different temperatures, 5, 10, 15, 20 and 25 °C, were processed. For each temperature we performed a three parameter minimisation using the downhill simplex method [19]. The standard deviation, defined as $\sqrt{\Phi/\sum_n \Pi_n^2} \times 100$, was always less than 0.5%. The fits are presented in Fig. 5, plotted in the same coordinates as in ref. [2].

The obtained values of the equilibrium constant of dimerisation, $K(T)$, are shown in Table 2, where we give also the standard *free energy* of dimerisation, ΔF°:

$$\Delta F^\circ = \mu_{20} - 2\mu_{10} = -kT \ln K(T) , \qquad (5.1)$$

cf. Eq. (3.6). As known [16], from the temperature dependence of K one can determine the standard *energy* (heat) of the reaction, using van't Hoff relation

$$\Delta E^\circ = -\frac{d \ln K(T)}{d(1/kT)} \qquad (5.2)$$

Table 2 Calculated values of the equilibrium constant of dimerisation, $K(T)$, and the free energy of dimerisation, ΔF°

T, °C	$K(T)$, nm^2	ΔF°, kJ/mol
5	2.850	−2.421
10	2.710	−2.346
15	2.600	−2.290
20	2.509	−2.242
25	2.378	−2.146

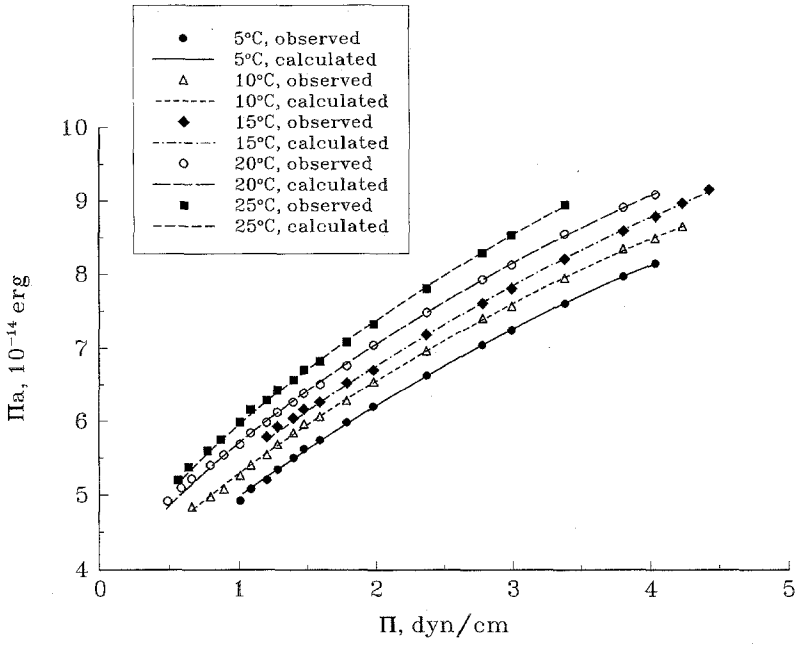

Fig. 5 Plots of the product (Πa) vs. Π for different temperatures. The symbols denote experimental data, taken from Fig. 5 in ref. [2], for *di*-C_{18}-lecithin at the *n*-heptane/aqueous NaCl interface. The theoretical curves are drawn in accordance with Eq. (3.8)

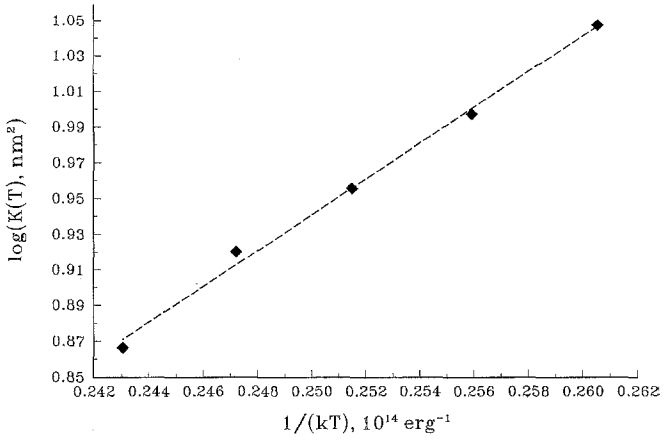

Fig. 6 Temperature dependence of the equilibrium constant of dimerisation, plotted in accordance with the van't Hoff equation, Eq. (5.2)

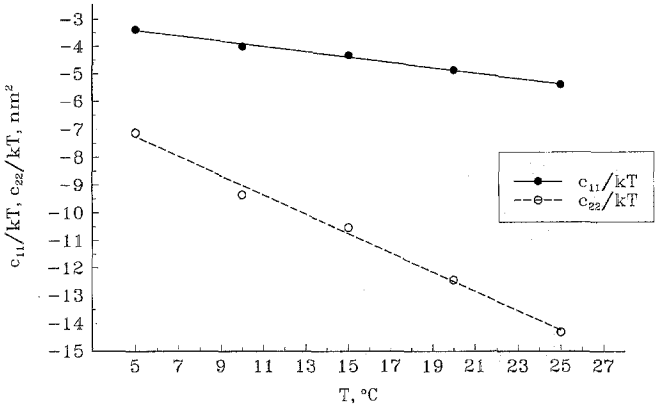

Fig. 7 Temperature dependence of the parameters characterising the monomer-monomer (c_{11}) and dimer–dimer (c_{22}) interactions

In Fig. 6 the data from Table 2 are presented in appropriate coordinates. The points lie on a straight line, which indicates that in the temperature interval under consideration the heat of dimerisation is constant. From the slope we find

$$\Delta E^{\circ} = -1.0 \times 10^{-13}\ \text{erg/molecule} = -6.0\ \text{kJ/mol}\ . \quad (5.3)$$

The process of dimer formation turns out to be slightly exothermic, with the heat being of the order of 2.5 kT per one pair of molecules. This finding supports the assumption put forward above concerning the shape of the potential curve of interaction between two lipid molecules (Fig. 4). The depth of the minimum in Fig. 4 can be identified as ΔE°.

Figure 7 shows the results for the two interaction parameters, c_{11} and c_{22}. Both are negative, which points to the dominating role of the repulsion in the integral interaction, see Fig. 4 and Eq. (2.7). Such repulsion between the normal components of neighbouring dipoles was found to have a considerable impact on the shape of condensed phase domains in lipid monolayers [20]. From Fig. 7 both c_{11} and c_{22} are seen to increase by absolute value with raising temperature. Qualitatively, this effect may be connected with the temperature dependence of the dielectric constant, cf. Eq. (4.4), as ε is known to fall down

with increasing T. However, one should keep in mind that the net normal dipole moment can also vary due to conformational or other structural (in particular, hydration) changes in the monolayer.

It is interesting to compare the magnitudes of c_{11} and c_{22}. If the normal dipole repulsion were the only source of interaction between lipids, and if the normal dipole moment of a dimer was exactly twice that of a monomer, then c_{11} would be given by expression analogous to Eq. (4.4), $c_{11} = -\pi p^2/(\varepsilon r_{11})$. Combining with Eq. (2.6), one would have obtained

$$c_{22} = 2\sqrt{2}\, c_{11} . \tag{5.4}$$

From the data in Fig. 7 it follows that c_{22} is slightly lower by absolute value than predicted by Eq. (5.4). This observation can be attributed to a normal dipole moment of dimers smaller than $2p$. Indeed, as mentioned above, a substantial part of the normal dipole moment is believed to be due to the oriented water molecules in the hydration shell around the lipid polar heads [12]. Then, it is natural to expect that the dipole moment originating from hydration of dimers should be a bit less than twice that which corresponds to monomers. Nevertheless, especially at higher temperature, the observed c_{22} is close to Eq. (5.4). We can consider this fact as an indication that assuming the dimer normal dipole moment to be of the order of $2p$ is qualitatively plausible. We used this assumption to determine c_{12} through Eq. (4.7).

Let us now discuss the composition of the monolayer, regarded as a mixture of monomers and dimers. Figure 8 presents the results for the molar fraction of dimers, x_2, calculated by means of Eqs. (3.10), (A4) and (A5). It is seen from Fig. 8 that even for fairly diluted monolayers the dimer content is appreciable. As the monolayer is compressed, x_2 generally increases. One can also consider the temperature dependence of x_2 at fixed area. The monolayer is insoluble and the total number of adsorbed lipid molecules, $N_1 + 2N_2$, is constant. That is why fixed a means also $A = \text{const.}$, cf. Eqs. (3.3) and (3.7). In these conditions the increased temperature favours dimerisation (Fig. 8). On the other hand, we found that the dimer formation is an exothermic process, Eq. (5.3). Consequently, one would expect dissociation of dimers with raising temperature. As shown below, the explanation of the observed reverse behaviour of x_2 is connected with the interactions in the monolayer.

It is known from thermodynamics (ref. [16], section 7.8) that the *standard* heat ΔE^0 and the corresponding $K(T)$, defined in terms of the standard chemical potentials, Eqs. (3.6) and (5.2), refer to an *ideal* system. In our case the equilibrium "constant", relevant for the real system with interactions between the particles, is represented by the quantity $K(T)\gamma_1^2/\gamma_2$:

$$K(T)\,\frac{\gamma_1^2}{\gamma_2} = a\,\frac{x_2(1+x_2)}{(1-x_2)^2} , \tag{5.5}$$

cf. Eqs. (3.6) and (3.8). In Fig. 9 we plot $K\gamma_1^2/\gamma_2$ as a function of a for different temperatures. γ_1 and γ_2 are given by Eq. (3.4). The data show that both compression of the monolayer at constant T, and increasing temperature at fixed a, favour dimerisation. Now the peculiar behaviour of the data for 5 °C in Fig. 8, which lie on a monotonic convex curve in Fig. 9, can be explained as influenced by the interactions. To understand physically the temperature dependence of x_2 we first note that, in general, the population of dimers increases when the magnitude of the energy

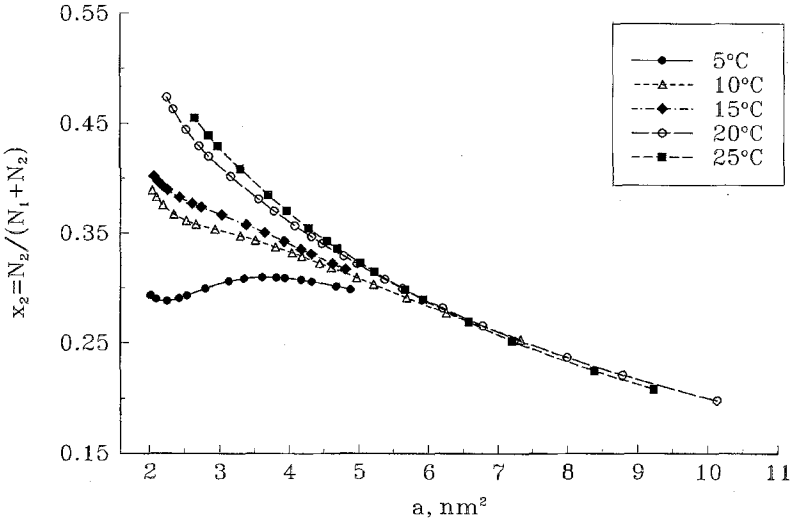

Fig. 8 Mole fraction of dimers in the lipid monolayer, x_2, calculated from Eqs. (3.10), (A4) and (A5), vs. the mean area per lipid molecule, a

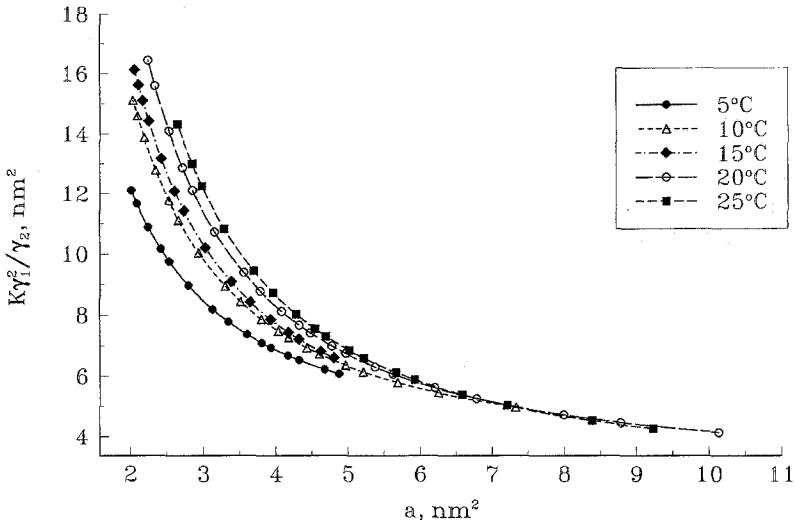

Fig. 9 Plot of the parameter $K(T)\gamma_1^2/\gamma_2$, characterising the chemical equilibrium in the real monolayer with interactions between the particles

of dimer formation, $|\Delta u|$, increases. At a finite area per molecule, a, this energy can be estimated as $|\Delta u| \approx u_{11}(\sqrt{a}) - u_{11}$ (min), where $\sqrt{a}$ is of the order of the average distance between two monomers, see Fig. 4. As mentioned above (see the discussion about Fig. 7), the long-range lipid–lipid repulsion (and consequently, $u_{11}(\sqrt{a})$) increases with the increase of temperature. Then $|\Delta u|$ and x_2 will also increase with T for fixed a.

Finally, we calculate the *real* heat of dimerisation in the monolayer, $\Delta E\ (a, T)$, accounting for the interparticle interactions. Thermodynamics gives us (ref. [16], Eq. (7.76))

$$\Delta E(a,T) = \Delta E^{\circ} - kT^2 \left(\frac{\partial \ln \gamma_2}{\partial T}\right)_{A,N_1,N_2} + 2kT^2 \left(\frac{\partial \ln \gamma_1}{\partial T}\right)_{A,N_1,N_2} . \tag{5.6}$$

It is possible to apply Eq. (3.4), which yields

$$\Delta E(a,T) = \Delta E^{\circ} + 2kT^2 \left\{ \Gamma_2 \left[\frac{d}{dT}\left(\frac{c_{22}}{kT}\right) - 2\frac{d}{dT}\left(\frac{c_{12}}{kT}\right)\right] + \Gamma_1 \left[\frac{d}{dT}\left(\frac{c_{12}}{kT}\right) - 2\frac{d}{dT}\left(\frac{c_{11}}{kT}\right)\right]\right\} . \tag{5.7}$$

Note that the deviation from ideality is due only to the long-range interaction accounted for by c_{ij} (b_{ij} are supposed to be temperature independent). The right hand side of Eq. (5.7) is calculated by using the results for x_2 and Γ, Eqs. (3.9), (3.10), (A2), (A4) and (A5). From Fig. 7, one obtains

$$\frac{d}{dT}\left(\frac{c_{11}}{kT}\right) = -0.09728\ \mathrm{nm}^2/K ,$$

$$\frac{d}{dT}\left(\frac{c_{22}}{kT}\right) = -0.3490\ \mathrm{nm}^2/K \tag{5.8}$$

and Eq. (4.7) gives

$$\frac{d}{dT}\left(\frac{c_{12}}{kT}\right) = -0.2044\ \mathrm{nm}^2/K . \tag{5.9}$$

The resulting values of $\Delta E(a, T)$ calculated according to Eq. (5.7) are plotted in Fig. 10 and compared with the heat of dimerisation in an ideal monolayer, ΔE°. In general, the repulsion between the particles decreases the exothermic heat effect of the reaction. As can be expected, the more compressed the monolayer, the higher the deviations from ideality. The energy of dimerisation in the real monolayer even changes sign and becomes *positive* (endothermic process) at low area per molecule and at higher temperature. At such conditions the heat effect of the long-range repulsion prevails over that of the reaction itself.

Concluding remarks

The lipid monolayers, when compressed, are known to form condensed phases with different organisation and structure [20, 21]. Before this happens, i.e. at relatively large area per molecule, it is likely that some small aggregates begin to form. Our work is devoted to investigation of this possibility. First we found out a clear indication that the relatively concentrated monolayers are built up from lipid dimers, see Fig. 2 and Table 1. In particular, the results show that the van der Waals equation can be used up to the very phase transition, which commences at $a = 75 - 100$ Å^2 depending on the temperature [1].

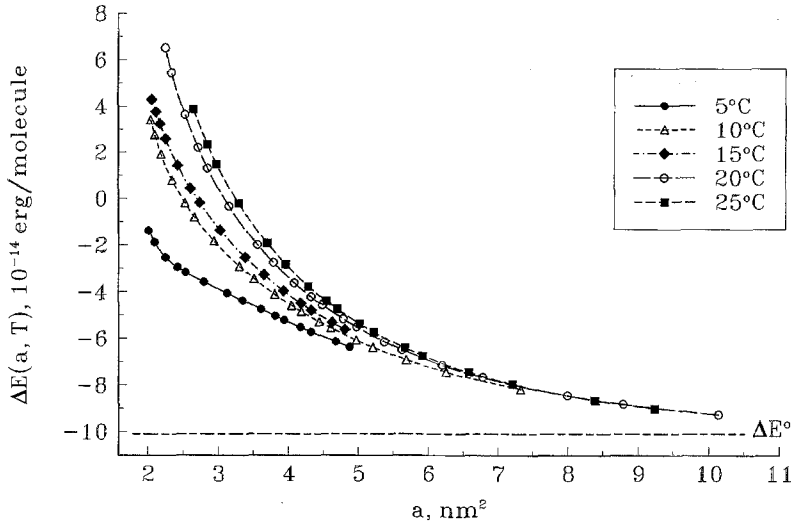

Fig. 10 Heat of dimerisation in a lipid monolayer with account for the interparticle interactions, $\Delta E(a, T)$, vs. the mean area per lipid molecule, a; ΔE° is the heat of dimerisation in an ideal monolayer

Then we examined more diluted monolayers, for area per molecule between 1000 and 200 Å^2. We developed a theoretical model regarding the monolayer as an equilibrium mixture of monomers and dimers, and accounting for the long-range interactions between the species. The model is based on the van der Waals equation of state, with the overall interaction constants b and c being composition dependent, see Eqs. (2.8)–(2.10). Statistical thermodynamics allows us to write expressions for the free energy and for the chemical potentials of the components. Thereby we find the amount of monomers and dimers in the layer and the corresponding activity coefficients. The model contains three adjustable parameters: the equilibrium constant of dimerisation and two interaction constants of type monomer–monomer and dimer–dimer. The model parameters are determined by fitting experimental $\Pi(a)$ isotherms for five different temperatures. From the values of the reaction constant we conclude that the process of dimerisation is slightly exothermic, with a heat of the order of 2.5 kT per one dimer. In addition, it is interesting to note that the dimerisation starts at very low surface concentrations, see Fig. 8.

Even without molecular interpretation the thermodynamic considerations are straightforward. However, one can go further and try to qualitatively rationalise the results in terms of the lipid structure. A simple molecular model (Fig. 1b) assigns net normal and lateral dipole moments to the lipid polar heads. The normal dipoles always repel each other giving rise to predominant overall repulsion (negative interaction constants c_{ij} in the equation of state). The lateral dipoles of the monomers supposedly rotate and only at close approach they can align antiparallel. The latter process leads to attraction and a dimer forms. This qualitative picture is consistent with our findings for the heat of dimerisation and for the interaction parameters.

We are aware of the fact that our treatment is indirect and, to some extent, model dependent. Nevertheless, we believe it reflects realistically the behaviour of the lipid monolayers. In addition, our results can help to distinguish the role of head–head and tail–tail interactions for the phase transition. The knowledge that the lipid molecules are coupled to form dimers may lead to a better understanding of the properties of condensed monolayers and lipid bilayers.

Acknowledgements This study was supported by the Research and Development Corporation of Japan (JRDC) under the Nagayama Protein Array Project of the Program "Exploratory Research for Advanced Technology" (ERATO). The authors are indebted to Prof. Ivan B. Ivanov for the most stimulating and encouraging discussions. We also acknowledge the help of Mr. Simeon Stoyanov, who carried out part of the numerical calculations, and Miss M. Paraskova, who typed the manuscript.

Appendix

Series expansions at low surface concentrations

The relation between the lipid total adsorption, Γ, and the average area per lipid molecule, a, reads

$$a^{-1} = (1 + x_2)\Gamma \tag{A1}$$

cf. Eq. (3.8). By substituting the expansions, Eqs. (3.9) and (3.10), into the right-hand side of Eq. (A1) and by comparing the coefficients that multiply identical powers of a^{-1} one derives

$$\Gamma_{(1)} = 1, \qquad \Gamma_{(2)} = -y_1, \qquad \Gamma_{(3)} = y_1^2 - y_2, \ \ldots \tag{A2}$$

Then the problem is reduced to finding the coefficients y_1, y_2, y_3, ... On that purpose it is convenient to represent the mass action law, Eq. (3.6), in the form

$$K\Gamma(1-x_2)^2\gamma_1^2(1-\Gamma b)=(1-\Gamma b)\gamma_2 x_2 \tag{A3}$$

By using Eqs. (2.9), (2.10), (3.4), (3.9) and (3.10) we expand γ_1, $(1-\Gamma b)\gamma_1$ and $(1-\Gamma b)\gamma_2$ in series for small a^{-1} and substitute the results in Eq. (A3). The comparison of the coefficients at equal powers of a^{-1} yields

$$y_1 = K,$$

$$y_2 = K[4(b_{11}-\tilde{c}_{11})-2(b_{12}-\tilde{c}_{12})-3K]\,, \tag{A4}$$

$$\begin{aligned} y_3 = K\Big\{ & 13K^2 + K[-32(b_{11}-\tilde{c}_{11}) \\ & + 20(b_{12}-\tilde{c}_{12}) - 2(b_{22}-\tilde{c}_{22})] \\ & + 2[2(b_{11}-\tilde{c}_{11}) - (b_{12}-\tilde{c}_{12})]^2 \\ & + \frac{7}{2}b_{11}^2 - 2b_{11}b_{12}\Big\} \end{aligned} \tag{A5}$$

where

$$\tilde{c}_{ij} = c_{ij}/(kT)\,.$$

Equations (A2), (A4) and (A5) determine the coefficients in Eqs. (3.9) and (3.10), which in turn allows the calculation of the $\Pi(a)$ isotherm by means of Eq. (3.8).

References

1. Yue BY, Jackson CM, Taylor JAG, Mingins J, Pethica BA (1976) J Chem Soc Faraday Trans I 72:2685–2693
2. Taylor JAG, Mingins J, Pethica BA (1976) J Chem Soc Faraday Trans I 72:2694–2702
3. Pethica BA, Mingins J, Taylor JAG (1976) J Colloid Interface Sci 55:2–8
4. Mingins J, Taylor JAG, Pethica BA, Jackson CM, Yue BY (1982) J Chem Soc Faraday Trans I 78:323–339
5. McDonald RC, Simon SA (1987) Proc Natl Acad Sci USA 84:4089–4091
6. Simon SA, McIntosh TJ, Magid AD (1988) J Colloid Interface Sci 126:74–83
7. Mingins J, Stigter D, Dill KA (1992) Biophys J 61:1603–1615
8. Dill KA, Stigter D (1988) Biochemistry 27:3446–3453
9. Stigter D, Dill KA (1988) Langmuir 4:200–209
10. Standish MM, Pethica BA (1968) Trans Faraday Soc 64:1113–1122
11. McIntosh TJ, Magid AD, Simon SA (1987) Biochemistry 26:7325–7332
12. Simon SA, McIntosh TJ (1989) Proc Natl Acad Sci USA 86:9263–9267
13. Landau LD, Lifshitz EM (1980) Statistical physics Part I Pergamon Press Oxford
14. Hill TL (1960) An introduction to statistical thermodynamics. Addison–Wesley Reading, Massachusetts
15. Heer CV (1972) Statistical mechanics, kinetic theory and stochastic processes Academic Press, London
16. Prigogine I, Defay R (1954) Chemical thermodynamics Longmans Green, London
17. Israelachvili JN (1992) Intermolecular and surface forces Academic Press, London
18. Kauzmann W (1957) Quantum chemistry Academic Press, New York
19. Press WH, Flannery BP, Tenkolsky SA, Vetterling WT (1987) Numerical recipes: the art of scientific computing. Cambridge University Press, Cambridge
20. Möhwald H (1990) Annu Rev Phys Chem 41:441–476
21. Thoma M, Möhwald H (1994) J Colloid Interface Sci 162:340–349